Corrections

CELL BIOLOGY

Correction for "Cell fate regulation by gelsolin in human gynecologic cancers," by Mohammad R. Abedini, Pei-Wen Wang, Yu-Fang Huang, Mingju Cao, Cheng-Yang Chou, Dar-Bin Shieh, and Benjamin K. Tsang, which appeared in issue 40, October 7, 2014, of *Proc Natl Acad Sci USA* (111:14442–14447; first published September 22, 2014; 10.1073/pnas.1401166111).

The authors note that the affiliation for Yu-Fang Huang and Cheng-Yang Chou should instead appear as Department of Obstetrics and Gynecology, National Cheng Kung University Hospital, College of Medicine, National Cheng Kung University, Tainan 704, Taiwan. The corrected author and affiliation lines appear below. The online version has been corrected.

Mohammad R. Abedini[a,b,c], Pei-Wen Wang[d], Yu-Fang Huang[e], Mingju Cao[a,b], Cheng-Yang Chou[e], Dar-Bin Shieh[d,f], and Benjamin K. Tsang[a,b]

[a]Departments of Obstetrics and Gynaecology and Cellular and Molecular Medicine, Interdisciplinary School of Health Sciences, University of Ottawa, Ottawa, ON, Canada K1H 8L6; [b]Chronic Disease Program, Ottawa Hospital Research Institute, Ottawa, ON, Canada K1H 8L6; [c]Cellular and Molecular Medicine Research Center, Department of Pharmacology, Birjand University of Medical Sciences, Birjand 97178, Iran; [d]Institute of Basic Medical Science, Institute of Oral Medicine and Department of Stomatology, National Cheng Kung University Hospital, College of Medicine, National Cheng Kung University, Tainan 704, Taiwan; [e]Department of Obstetrics and Gynecology, National Cheng Kung University Hospital, College of Medicine, National Cheng Kung University, Tainan 704, Taiwan; and [f]Advanced Optoelectronic Technology Center and Center for Micro/Nano Science and Technology, National Cheng Kung University, Tainan 704, Taiwan

www.pnas.org/cgi/doi/10.1073/pnas.1421407111

CELL BIOLOGY

Correction for "Evidence for multiple roles for grainyheadlike 2 in the establishment and maintenance of human mucociliary airway epithelium," by Xia Gao, Christopher M. Vockley, Florencia Pauli, Kimberly M. Newberry, Yan Xue, Scott H. Randell, Timothy E. Reddy, and Brigid L. M. Hogan, which appeared in issue 23, June 4, 2013, of *Proc Natl Acad Sci USA* (110:9356–9361; first published May 20, 2013; 10.1073/pnas.1307589110).

The authors note that the title appeared incorrectly. The title should instead appear as "Evidence for multiple roles for grainyhead-like 2 in the establishment and maintenance of human mucociliary airway epithelium." The online version has been corrected.

www.pnas.org/cgi/doi/10.1073/pnas.1421315111

ECOLOGY

Correction for "Biogeographic variation in evergreen conifer needle longevity and impacts on boreal forest carbon cycle projections," by Peter B. Reich, Roy L. Rich, Ying-Ping Wang, and Jacek Oleksyn, which appeared in issue 38, September 23, 2014, of *Proc Natl Acad Sci USA* (111:13703–13708; first published September 15, 2014; 10.1073/pnas.1216054110).

The authors note that on page 13705, left column, second full paragraph, lines 11 and 12, "foliage and roots represent a greater and smaller fraction, respectively, of total biomass in forests in increasingly cold environments (26)" should instead appear as "foliage and roots represent a smaller and greater fraction, respectively, of total biomass in forests in increasingly cold environments (26)."

www.pnas.org/cgi/doi/10.1073/pnas.1421130111

Evidence for multiple roles for grainyhead-like 2 in the establishment and maintenance of human mucociliary airway epithelium

Xia Gao[a], Christopher M. Vockley[a], Florencia Pauli[b], Kimberly M. Newberry[b], Yan Xue[a], Scott H. Randell[c], Timothy E. Reddy[d,e,1], and Brigid L. M. Hogan[a,1]

[a]Department of Cell Biology, [d]Department of Biostatistics and Bioinformatics, and [e]Institute of Genome Sciences and Policy, Duke University, Durham, NC 27710; [b]HudsonAlpha Institute for Biotechnology, Huntsville, AL 35806; and [c]Department of Cell Biology and Physiology, University of North Carolina at Chapel Hill School of Medicine, Chapel Hill, NC 27599

Contributed by Brigid L. M. Hogan, April 23, 2013 (sent for review March 7, 2013)

Most of the airways of the human lung are lined by an epithelium made up of ciliated and secretory luminal cells and undifferentiated basal progenitor cells. The integrity of this epithelium and its ability to act as a selective barrier are critical for normal lung function. In other epithelia, there is evidence that transcription factors of the evolutionarily conserved grainyheadlike (GRHL) family play key roles in coordinating multiple cellular processes required for epithelial morphogenesis, differentiation, remodeling, and repair. However, only a few target genes have been identified, and little is known about GRHL function in the adult lung. Here we focus on the role of GRHL2 in primary human bronchial epithelial cells, both as undifferentiated progenitors and as they differentiate in air–liquid interface culture into an organized mucociliary epithelium with transepithelial resistance. Using a dominant-negative protein or shRNA to inhibit GRHL2, we follow changes in epithelial phenotype and gene transcription using RNA sequencing or microarray analysis. We identify several hundreds of genes that are directly or indirectly regulated by GRHL2 in both undifferentiated cells and air–liquid interface cultures. Using ChIP sequencing to map sites of GRHL2 binding in the basal cells, we identify 7,687 potential primary targets and confirm that GRHL2 binding is strongly enriched near GRHL2-regulated genes. Taken together, the results support the hypothesis that GRHL2 plays a key role in regulating many physiological functions of human airway epithelium, including those involving cell morphogenesis, adhesion, and motility.

The lung is composed of a highly branched, tree-like system of tubes ending in millions of alveoli for gas exchange. Most of the conducting airways of the human lung are lined by an epithelium made up of ciliated and secretory luminal cells and undifferentiated basal progenitors (1, 2). This layer fulfills many critical physiological functions, including mucociliary clearance and innate host defense, and provides a barrier against pathogens and allergens. The luminal cells are highly polarized, and their lateral membranes contain specialized junctional domains that mediate adhesion and the selective transcellular passage of ions, molecules, and immune cells (3). Junctional complexes are connected to the cytoskeleton and form part of an integrated system maintaining epithelial integrity. Many of the components of this system in the human lung are evolutionarily conserved and function in other tubular systems (4), but we are still far from a complete "systems biology" of the airway epithelium.

There are many reasons why such a goal is clinically relevant. Defects in airway barrier function may increase susceptibility to infection and inflammation, and underlie some aspects of disorders such as asthma and chronic obstructive pulmonary disease (5–7). There is also evidence that defects in the ability of basal cells to regenerate an intact epithelium after damage promote airway fibrosis (8). One way to uncover a gene regulatory network governing the integrity of the airway epithelium is to identify key regulators governing multiple downstream targets. Candidates for this role include members of the conserved grainyheadlike (GRHL) family of transcription factors. These are known to control many aspects of epithelial behavior, including cell polarity, motility, morphogenesis, transcellular transport, lipid metabolism, differentiation, and wound healing in multiple tissues and species from *Drosophila* to human (9–14). In the embryonic mouse lung, *Grhl1–3* genes exhibit differential spatiotemporal patterns of expression in the epithelium (15, 16). Recent analysis of *Grhl2* mutants, which die around embryonic day 11.5 from neural tube closure defects, indicates that the gene plays a role in lung branching morphogenesis (17). In addition, recent studies with mouse lung alveolar-like cell lines in culture strongly support a role for *Grhl2* in cell adhesion, motility, and junction formation and identify a number of likely primary targets (16). However, there has been no systematic study of GRHL proteins in primary human bronchial epithelial (HBE) cells or genome-wide analysis of their potential regulatory sites.

Here we show that GRHL genes are differentially expressed in human airways and HBE cells differentiating into a mucociliary epithelium (18). Using a dominant-negative mutant protein and shRNA, we demonstrate that GRHL2 is required for the establishment and maintenance of epithelial barrier function and regulates several hundreds of genes in basal and differentiated cells. ChIP-seq (sequencing) experiments identify several thousand potential primary targets in basal cells and confirm that GRHL2 binding is strongly enriched near GRHL2-regulated genes. Taken together, our results provide evidence that GRHL2 is a critical component of the gene regulatory network of human airway epithelium.

Results

GRHL Protein Expression in Human Airways and HBE Cells in Culture. In the normal human lung, immunohistochemistry (IHC) of sections of small and large airways shows GRHL2 in the nuclei of both luminal and p63$^+$ KRT5$^+$ basal cells. By contrast, GRHL1 is expressed predominantly in MUC5AC$^+$ goblet cells and GRHL3 in acetylated tubulin$^+$ ciliated cells (Fig. 1 *A–E*).

The in vitro culture of primary HBE cells presents a convenient method for testing the function of GRHL proteins in airway epithelium. When cultured in plastic dishes submerged in growth medium, all cells remain undifferentiated and express the basal markers p63 and KRT5. Even when confluent, they

Author contributions: X.G., C.M.V., S.H.R., T.E.R., and B.L.M.H. designed research; X.G., C.M.V., F.P., K.M.N., and Y.X. performed research; X.G., C.M.V., T.E.R., and B.L.M.H. analyzed data; and X.G., C.M.V., T.E.R., and B.L.M.H. wrote the paper.

The authors declare no conflict of interest.

Freely available online through the PNAS open access option.

Data deposition: The data reported in this paper have been deposited in the Gene Expression Omnibus (GEO) database, www.ncbi.nlm.nih.gov/geo (accession nos. GSE46194, GSE44718, and GSE44809).

[1]To whom correspondence may be addressed. E-mail: tim.reddy@duke.edu or brigid.hogan@duke.edu.

This article contains supporting information online at www.pnas.org/lookup/suppl/doi:10.1073/pnas.1307589110/-/DCSupplemental.

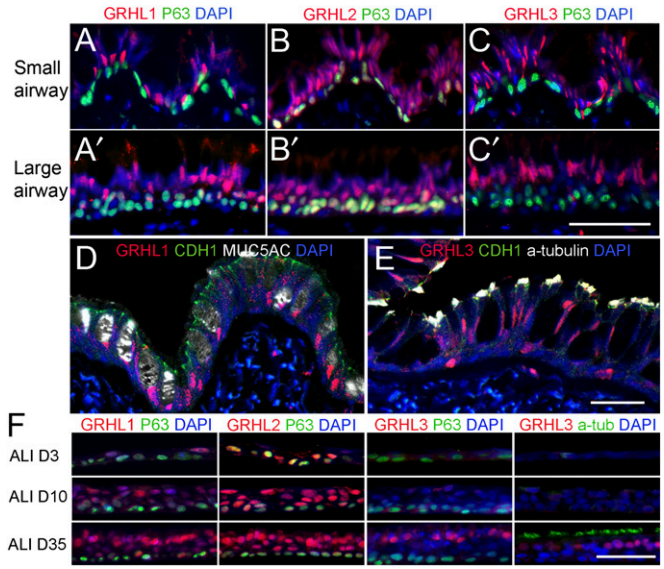

Fig. 1. GRHL proteins in human airway cells. (*A*–*C*′) IHC of small and large human airways (1- and 6-mm diameter, respectively) for GRHL1, 2, and 3 (red), p63 (green), and DAPI (blue). (*D* and *E*) Small airways showing GRHL1 and 3 (red), E-cadherin (CDH1) (green), α-tubulin, a ciliated cell marker (white), MUC5AC, a marker for goblet cells (white), and DAPI (blue). Single images are from confocal stacks. (*F*) IHC for GRHL1, 2, and 3 and airway cell-specific markers of sections of HBE cultures at ALI D3, D10, and D35. (Scale bars, 50 μm.)

have very few intercellular junctions containing TJP1 (ZO-1). The cells robustly express nuclear GRHL2, but have low levels of GRHL1 and no detectable GRHL3. By contrast, when transferred to air–liquid interface (ALI) culture in differentiation medium, the cells differentiate into a mucociliary epithelium in about 4 wk. In the initial 3–7 d after seeding, most cells are still undifferentiated and express p63, KRT5, and GRHL2, with lower levels of GRHL1 (Fig. 1*F*, *Top*). When confluent, the cells now express obvious intercellular junctions with TJP1 and Claudin 4 (CLDN4) (see Fig. 3*B*). By ALI day (D) 10, $p63^-$ nuclei are seen above the $p63^+$ basal layer and GRHL1 is present at higher levels in these suprabasal nuclei (Fig. 1*F*, *Middle*). Only by ALI D35, when differentiated ciliated and secretory cells are present, is GRHL3 detectable in ciliated cells (Fig. 1*F*, *Bottom*).

GRHL2 Regulates the Expression of Multiple Genes in Undifferentiated HBE Cells. We used RNA-seq to identify genes regulated by GRHL2 in undifferentiated HBE cells from three human donors (Fig. 2*A*). Specifically, we identified transcripts differentially expressed 24 h after inhibiting GRHL function with an inducible lentivirus driving a dominant-negative (DN) mutant form of the protein (Fig. S1). This DN-GRHL2 protein, in which the N-terminal transactivating domain is replaced with EGFP, is identical to a mouse DN-GRHL2 mutant protein previously shown to displace GRHL2 from a known target site in the *Cdh1* gene and to block its transcription (9). Control virus expressed nuclear H2B-GFP.

There were 980 unique genes differentially expressed in the DN-GRHL2 vs. control cells with an adjusted *P* value <0.05 and an average change in expression greater than 50% (Dataset S1). A similar proportion of genes was up- ($n = 523$) and down-regulated ($n = 457$) (Fig. 2*B*). Annotating the differentially expressed genes with the Gene Ontology suggests that GRHL2 regulates diverse functions in undifferentiated HBE cells, including those associated with morphogenesis, adhesion, and migration. In addition, GRHL2-regulated proteins were significantly more likely to be localized to the cell periphery, especially the apical and apicolateral membranes ($P = 7.5 \times 10^{-3}$ and $P = 6.9 \times 10^{-3}$, respectively). Full Gene Ontology enrichments are shown in Dataset S2.

Some genes differentially expressed in response to DN-GRHL2 may lie downstream of direct targets, including microRNAs (19). Therefore, to identify direct GRHL2 targets, we performed ChIP-seq on HBE cells grown under the same conditions as for the RNA-seq studies. There were 7,687 GRHL2 binding sites reproducibly identified among all the three donors (Dataset S3). The sites were enriched for the known GRHL2-binding motif (Fig. 2*C*) and included the few genes that had been shown from previous ChIP studies to have GRHL2 binding sites [e.g., *CLDN4* and *CDH1* (9, 16)]. Representative sites for *MPZL2*, *KRT5*, *SEMA4B*, and *HMBB1* are shown in Fig. 2*E*. Functional annotation analysis of all genes near GRHL2 binding sites using GREAT (20) reveals a specific enrichment for binding near genes involved both in epithelial cell–cell adhesion [false discovery rate (FDR), 5.2×10^{-8}] and in cell–matrix adhesion [false discovery rate, 9.7×10^{-4}].

Genes that were differentially expressed with DN-GRHL2 were enriched for nearby GRHL2 binding, particularly within 40 kb of the transcription start site (Fig. 2*D* and Fig. S2*A*), suggesting that those genes are direct targets of GRHL2. Based on this analysis, we considered genes that are both regulated by DN-GRHL2 and bound by GRHL2 within 40 kb of the transcription start site to be direct targets ($n = 296$). These genes were significantly more likely to have reduced expression after DN-GRHL2 (206 vs. 90; $P = 7 \times 10^{-29}$ using a two-sided Fisher's exact test). More generally, the proportion of genes with reduced expression after DN-GRHL2 directly and significantly correlated with the proximity of GRHL2 binding to the transcription start site (Spearman's $\rho = 0.09$, $P < 1 \times 10^{-57}$; Fig. S2 *B* and *C*).

Clearly, there are many more GRHL2 binding sites in the genome than genes modulated over 24 h in undifferentiated HBE cells in response to DN-GRHL2. Therefore, to better understand the specific function of candidate direct targets, we repeated the functional enrichment analysis using only differentially expressed genes with GRHL2 binding within 40 kb of the transcription start

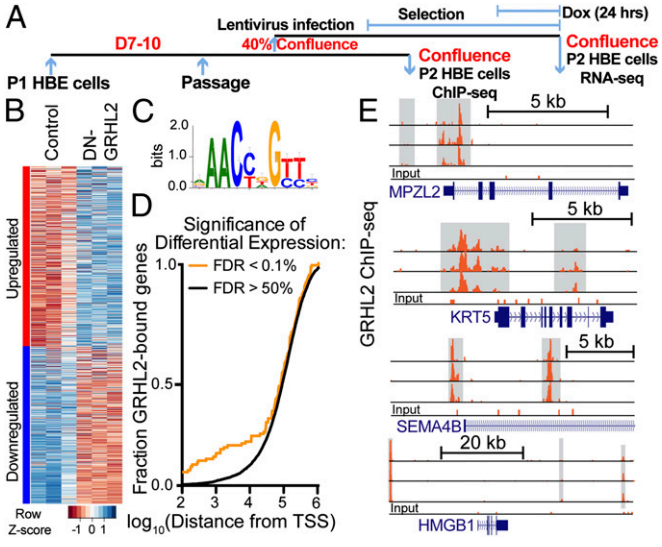

Fig. 2. ChIP-seq and RNA-seq experiments. (*A*) Schematic for growing, infecting, and harvesting primary HBE cells. (*B*) Relative expression of the 980 genes (rows) differentially expressed in response to DN-GRHL2. Log-transformed expression levels were normalized on a per-gene basis. (*C*) The GRHL2-binding motif identified in our GRHL2 ChIP-seq using de novo motif discovery. (*D*) The fraction of genes with GRHL2 binding (*y* axis) within the indicated distance of the transcription start site (TSS) (x axis). The orange and black lines are differentially and not differentially expressed genes, respectively, at the indicated FDR. (*E*) Examples of GRHL2 binding sites found near GRHL2-regulated genes.

site (Dataset S4). These genes were specifically enriched in multiple functional categories. Examples include those related to multicellular organismal development (morphogenesis) (*SEMA4A/B, CTNNBIP1, GJB5*, *TGM1*, *MPZL2, COL7A1, OVOL2*, and *GPR56* were among those down-regulated by DN-GRHL2), hemidesmosome assembly (*LAMA3* and *KRT5*), and cell "motility" (*VEGFA, EPHA1, HMGB1, SUN2, NRP2*, and *PDGFA* were down-regulated and *KDR* and *PRKD2* were up-regulated). The last category includes genes that are likely involved in epithelial-to-mesenchymal signaling (*KDR, VEGFA, HMGB1*, and *PDGFA*).

GRHL2 Is Required to Establish Barrier Function and Differentiation of HBE Cells in ALI Culture. After transfer to ALI culture, undifferentiated HBE cells give rise to a well-differentiated, polarized mucociliary epithelium with transepithelial resistance (TER). To evaluate the role of GRHL2 in the formation of this epithelium, we used the doxycycline (Dox)-inducible DN-GRHL2 lentivirus system to inhibit protein function from the time the cells first reach confluence (around ALI D7) (Fig. 3*A*). At this time, the cultures have distinct apical junctional complexes and localized CDH1, CLDN4, and TJP1 (Fig. 3*B*). In the experiment shown in Fig. 3*C*, TER began to increase in control cultures at D11 and reached a plateau around D18. However, following induction of DN-GRHL2, the cultures completely failed to establish TER (Fig. 3*C*). By ALI D14, although the number and density of cells on the membranes were essentially the same, cells expressing DN-GRHL2 (visualized by GFP staining) expressed much lower levels of CDH1, CLDN4, and TJP1 than controls (Fig. 3*D*). Significantly, CDH1 and TJP1 proteins had a more punctate distribution. In the case of TJP1, the protein was often localized in the nucleus, suggesting that inhibition of GRHL function interferes with the shuttling of TJP1 between the nucleus and cell membrane (21).

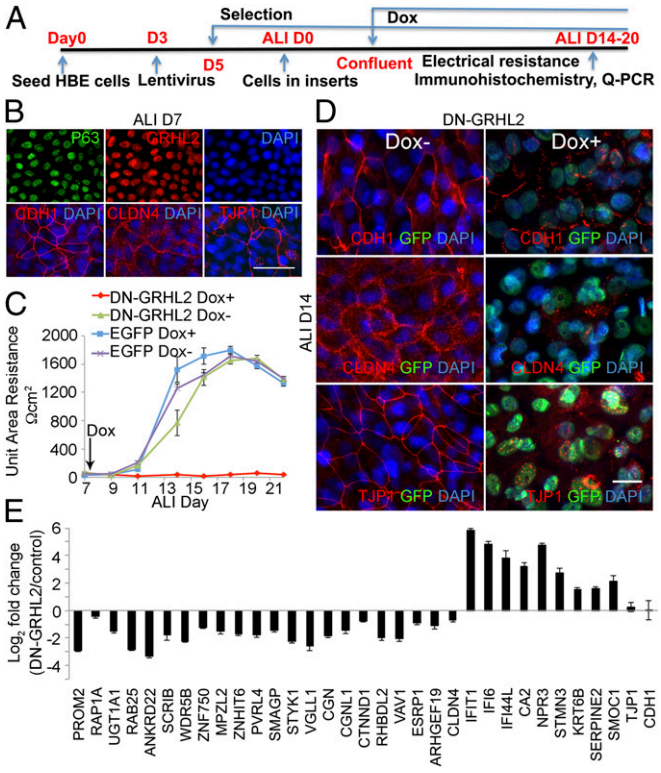

Fig. 3. DN-GRHL2 in HBE cells impairs establishment of barrier function. (*A*) Schematic of infection, selection, and expression of DN-GRHL2 and control H2B-GFP using TRIPZ lentivirus induced in confluent cultures at ALI D7. (*B*) Whole-mount IHC of cells at ALI D7 for junction proteins [CDH1, CLDN4, and TJP1 (ZO-1)], GRHL2, and p63. All cells express GRHL2 and most are p63^{+}. (*C*) Dox was added after cells reached confluence at ALI D7. Controls received no Dox. Values are averages and SEM of triplicate wells and the data are from one of $n = 3$ biological replicates. (*D*) Whole-mount IHC of DN-GRHL2 cultures with and without Dox at ALI D14 for junction proteins CDH1, CLDN4, and TJP1 (red) and GFP (green). Note that many cells expressing DN-GRHL2 have nuclear TJP1. (*E*) qPCR verification of genes differentially expressed in microarray analysis. Values are average and SEM of samples analyzed in triplicate from two biological replicates. (Scale bars, 20 μm.)

To confirm the specificity of the effect of DN-GRHL2 on HBE cells in ALI culture, we used the same lentiviral protocol to induce expression of an shRNA against GRHL2, with red fluorescent protein (RFP) as a reporter. Control Western blot and quantitative (q)PCR experiments at ALI D28 established that this shRNA reduced protein and RNA levels by 64% and 75%, respectively, compared with scrambled shRNA (Fig. 4*A*). Even though inhibition of GRHL2 protein levels was not complete, Fig. 4*B* shows that GRHL2 shRNA inhibited the development of TER compared with control RNA, with a statistically significant difference in levels at ALI D21/22. Moreover, RFP^{+} cells within the cultures that express GRHL2 shRNA do not differentiate into ciliated or secretory cells at ALI D28 (Fig. 4*B*). Taken together, these results are further evidence that GRHL2 is required for the de novo establishment of barrier function and the differentiation of primary HBE cells.

Returning to the experiments using DN-GRHL2, we used Affymetrix microarray analysis to identify transcriptional changes induced by inhibiting GRHL2 function between ALI D7 and D14 (Dataset S5). We found 607 unique genes that had a significant change in expression between cells expressing DN-GRHL2 versus EGFP ($P < 0.05$; absolute fold change in expression >1.5). Of those, 258 (43%) had lower expression, whereas 349 (57%) had increased expression. The changes were highly concordant with the results of DN-GRHL2 expression in undifferentiated HBE cells, with 72% of genes regulated in the same direction. Of the 61 genes with significant differential expression in both experiments, 92% were regulated in the same direction. Genes with lower expression after DN-GRHL2 during ALI D7–14 were strongly enriched in the GRHL2 binding sites that we documented in undifferentiated HBE cells, suggesting that a subset of the same GRHL2 binding sites is functional in the ALI D7–14 cells. Of the 258 down-regulated genes, 125 (48%) had GRHL2 binding within 40 kb of the transcription start site. In comparison, only 77 (22%) of the up-regulated genes had GRHL2 binding sites. As in the undifferentiated HBE cells, the relative enrichment of genes with reduced expression after DN-GRHL2 was stronger for GRHL2 binding sites located closer to the transcription start site. This further suggests that GRHL2 binding primarily increases expression of nearby genes.

We used qPCR to confirm the down-regulation of some of the most highly differentially expressed genes, as well as other genes selected for their known involvement in epithelial functions and for having occupied GRHL2 sites in HBE cells (Fig. 3*D*). These included known targets of GRHL2 in other tissues (*CLDN4* and *ARHGEF19*), even though the relative decreases in these genes in the microarray (~1.4-fold) were just below the cutoff for inclusion in Dataset S5. The confirmed genes encode proteins that fall into a number of different classes, including membrane-associated proteins such as PROM2, RHBDL2 [a membrane-associated protease up-regulated in epidermal cells undergoing wound repair (22)], SMAGP [small trans-membrane and glycosylated protein (23)], STYK1 [a novel membrane-associated tyrosine kinase (24)], and SCRIB [implicated in planar cell polarity and epidermal wound repair (25)]. Another class encompasses small GTPases and other adaptor proteins, including RAB25 [associated with the recycling of membrane proteins and in GRHL2 function (13)], RAP1A (a Ras-related protein active in cell locomotion), and VAV1 [a Rho-GEF implicated in barrier function in colon epithelium (26)]. A third class includes proteins connected with cell adhesion, including CGN, CGNL1, CTNND1, MPZL2 [also known as epithelial V-like antigen (EVA1) and

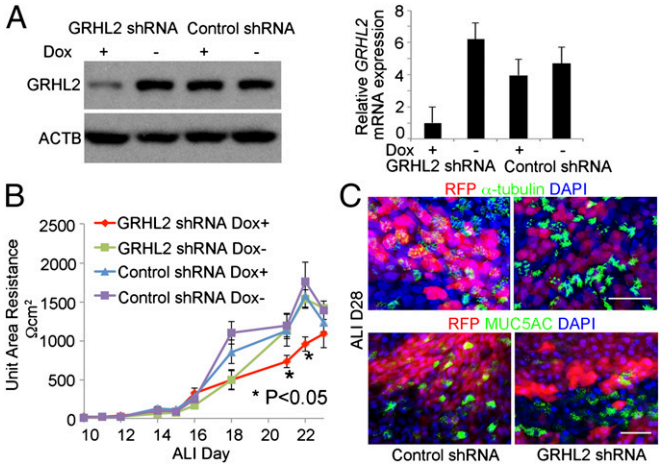

Fig. 4. GRHL2 shRNA inhibits barrier formation and differentiation of HBE cells. The protocol for induction of GRHL2 shRNA and control scrambled RNA was as for Fig 3. (*A*) (*Left*) Western blot of extracts of ALI cultures treated with Dox between D7 and D28 shows that GRHL2 shRNA reduced protein levels by 64% compared with control shRNA. ACTB, β-actin loading control. (*Right*) qPCR shows a corresponding 75% reduction of *GRHL2* transcript levels. Values are average and SEM of triplicates. (*B*) Values for TER are averages and SEM of triplicate wells and data are from one of $n = 2$ biological replicates. (*C*) At ALI D28, cultures were stained in whole-mount for α-tubulin, MUC5AC, and DAPI. RFP-positive cells express shRNA. Cells that express GRHL2 shRNA do not differentiate. (Scale bars, 50 μm.)

implicated in barrier formation between Sertoli cells (27) and as a target of Grhl2 in mouse embryonic neurectoderm (17)], and PVRL4 [poliovirus receptor-related 4, also known as nectin4, required for adherens junction formation in skin (28)]. Finally, we confirmed down-regulation of genes encoding ESRP1, an epithelial spicing regulatory protein (29), and various transcription factors and cofactors, including VGLL1 (30), WDR5B [a protein closely related to WDR5, a core component of the Trithorax histone methyltransferase complex that interacts with GRHL3 in keratinocyte differentiation (10)], ZNF750 [associated with the differentiation and development of barrier function of keratinocytes (31)], and ZNHIT6 [zinc finger protein implicated in RNA processing and emphysema (32)].

As shown in Fig. 3*D*, qPCR also confirmed the differential expression of transcripts for genes most highly up-regulated in the array. All except IFIT1, IFI6, and IFI44L (which encode IFN-inducible proteins) have occupied GRHL2 binding sites in basal cells. They were *CA2*, *KRT6B*, *NPR3* (natriuretic peptide receptor 3), *SERPINE2* (a peptidase inhibitor), *SMOC1* (SPARC-related modular calcium binding 1), and *STMN3* (also known as *SCLIP*, encoding a member of a family of proteins that destabilizes microtubules and promotes the motility of non-small-cell lung cancer cells (33).

Finally, the qPCR analysis confirmed that there was no change in the level of transcripts for the junction proteins CDH1 and TJP1 (Fig. 3*D*), even though these genes have distinct GRHL2 binding by ChIP-seq analysis of basal cells and CDH1 has been identified as a direct target in other cell types.

GRHL2 Is Required to Maintain Barrier Function in ALI Cultures. We next asked whether GRHL2 is required to maintain the integrity of the epithelium once barrier function has been established. To achieve this, Dox was added to cells transfected with either DN-GRHL2 or H2B-GFP virus at a time when TER values had reached a maximum (Fig. 5*A*). In the experiment shown in Fig. 5*B*, TER starts to decline 48 h after adding Dox and 7–10 d later reaches a new lower baseline. At this time, control cultures have a cobblestone epithelial appearance (Fig. 5*C*). By contrast, cells expressing DN-GRHL2, although still confluent, appear more extended and less closely adherent to each other. This difference in morphology is reflected in histological sections of the coherent epithelial layer (Fig. 5*D*). There was no evidence for significant cell death (by staining for cleaved caspase 3) or for a difference in proliferation (Ki67 staining, Fig. 5*E*) between control and experimental cultures.

To identify GRHL-regulated genes, we treated ALI cultures transfected with either H2B-GFP or DN-GRHL2 virus with Dox when the TER reached a threshold level (between ALI D14 and D18, depending on the donor). RNA was isolated from cultures harvested just 48 h later to focus on early events in the uncoupling of junctional interactions, including those regulating TER. We found 94 unique genes expressed at lower levels and 209 expressed at higher levels in cells expressing DN-GRHL2 compared with control ($P < 0.05$; absolute fold change >1.5; Dataset S6). Again, genes expressed at lower levels were much more likely to have previously identified GRHL2 binding sites close to the transcription start site than genes expressed at higher levels (65% vs. 19% for GRHL2 binding within 40 kb). Genes with significant differential expression after DN-GRHL2 expression during ALI D7–14 and ALI D14–18 were highly concordant between the two experiments (Spearman's $\rho = 0.88$). For no genes reaching our significance criteria did the expression level after DN-GRHL2 expression change in opposite directions. qPCR was used to confirm the down-regulation of the same set of genes down-regulated in cultures treated with Dox at ALI D7 (Fig. 5*F*).

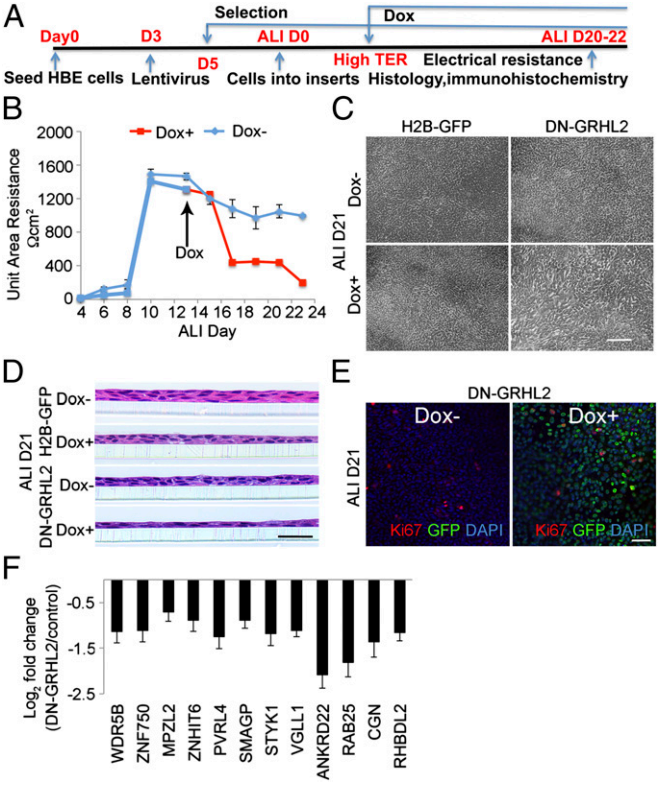

Fig. 5. DN-GRHL2 disrupts established barrier function in HBE cells. (*A*) Schematic of infection, selection, and induction of DN-GRHL2 when cultures had attained their high electrical resistance. (*B*) After induction of DN-GRHL2 at ALI D13, the TER of HBE cultures decreased compared with controls without induction or with H2B-GFP (not shown). Samples analyzed as in Fig. 3*B*. (*C* and *D*) Bright-field images and hematoxylin and eosin-stained sections of control H2B-GFP and DN-GRHL2–expressing cells on inserts at ALI D21. (*E*) Whole-mount IHC of control H2B-GFP and DN-GRHL2 cultures using Ki67 showed no difference in cell proliferation. (*F*) qPCR verification of genes differentially expressed in microarray analysis. Values as in Fig. 3*E* from $n = 3$ biological samples. (Scale bars, 10 μm.)

Finally, we identified genes specifically regulated by DN-GRHL2 in undifferentiated HBE cells compared with cells that are both establishing and maintaining transepithelial resistance in ALI culture. The analysis confirmed that only a small fraction of genes was specifically regulated by DN-GRHL2 between progenitor cells and cells in ALI culture (Fig. S2*D* and Dataset S7).

Discussion

Taken together, our studies provide compelling evidence that GRHL transcription factors and their downstream targets play important roles in the mucociliary epithelium of the human lung. In particular, the ChIP-seq studies unequivocally establish in an epithelial cell type that GRHL2 binds near thousands of genes encoding proteins involved in multiple cellular processes, many of which are common to epithelial cells in general. It appears that GRHL2 most frequently functions in HBE cells to positively regulate gene transcription. There is also evidence that it directly or indirectly has a role in transcriptional repression. In addition, GRHL2 may function as a "placeholder," helping to keep a subset of unexpressed genes poised for the later assembly of additional regulatory factors in cell types derived from the basal cells. Further experiments are necessary to distinguish between these possibilities.

A central strategy of this study was to identify genes regulated by GRHL2 in primary HBE cells at different stages of differentiation, in basal progenitors, or in cells in ALI culture establishing barrier function and differentiating into ciliated and secretory cells. At each stage it appears that expression of DN-GRHL2 leads to the down- or up-regulation of several hundreds of genes. Not all potential direct targets are affected, for at least two potential reasons. First, DN-GRHL2 may not be fully effective in occupying GRHL2 sites, or in displacing wild-type protein that is tightly bound. Second, even when the mutant protein is present and bound, other factors associated with particular genes may compensate for the lack of GRHL2 transactivation function. Nevertheless, it appears that GRHL2 does regulate a large set of genes common to all three stages of differentiation, in particular those related to epithelial morphogenesis, adhesion, and locomotion. The precise in vivo function of most of these genes remains to be determined. There is experimental evidence that several of them (e.g., MPZL2, PVRL4, RHBDL2, VAV1, and ZNF750) play a role in epithelial barrier function, wound repair, and pathology in other tissues. This suggests that we have uncovered a set of genes that could potentially mediate important functions relevant to airway health and disease. One strategy to define these functions will be to conditionally manipulate them in the mouse trachea, a model for the human mucociliary epithelium with basal cells (1).

Finally, our data provide evidence for considerable complexity in the mechanisms by which GRHL2 regulates functions such as intercellular adhesion in HBE cells. For example, inhibiting GRHL2 function in cells between ALI D7 and D14 leads to the absence of the discrete localization of TJP1 protein in apical junctional complexes. However, TJP1 protein is still present in the cells, albeit in a punctate pattern in the cytoplasm and nucleus. GRHL2 binds to the promoter region of *TJP1*, but there is apparently no change in RNA levels in response to DN-GRHL2. This suggests that other genes that are directly regulated by GRHL2 indirectly affect processes such as junction assembly and cell polarity at the posttranscriptional or posttranslational level. Potential mechanisms include alternative splicing of transcripts by ESRP1/2 [epithelial splicing regulatory proteins (29)], trafficking of membrane components through RABs, and dynamic interaction of membrane proteins with the cytoskeleton mediated by multiple ARHGEF and ARHGAP family members. Defining the precise hierarchy of mechanisms by which GRHL2 affects epithelial behavior and how these intersect with other regulatory networks will require multiple lines of investigation.

Materials and Methods

Cell Culture. Primary HBE cells were obtained from donors without preexisting lung disease under University of North Carolina at Chapel Hill Biomedical IRB protocol #03-1396. ChIP-seq and RNA-seq experiments used the same three donors. Passage (P) 1 P1 cells were seeded into plastic dishes coated with bovine collagen (Advanced BioMatrix; PureCol, 5005-B) in BEGM Basal Epithelial Growth Medium (34) containing 0.11 mM Ca^{2+} and 25 ng/mL EGF (34). Confluent cultures were passaged to P2 in dishes without collagen. For ChIP-seq, P2 cells were collected at confluence. For RNA-seq, P2 cells at 40% confluence were infected with H2B-GFP or DN-GRHL2 lentivirus and 1 μg/mL puromycin was added 48 h later. At confluence, 0.5 μg/mL Dox was added for 24 h.

For ALI cultures, P0 HBE cells were seeded in collagen-coated 10-cm dishes. At 40% confluence, cultures were infected with lentivirus and grown for 48 h before puromycin selection. At 70–90% confluence, 1.25×10^5 cells were seeded onto collagen IV (Sigma-Aldrich; C7521)-coated 12-mm Transwell permeable supports (Corning; 3460) in ALI culture medium (formula is given in ref. 34) with 1 mM Ca^{2+} and 0.5 ng/mL EGF. Medium was changed three times a week. Triplicate inserts were washed and 500 μL ALI medium was added before measuring TER every other day using a Millicell ERS2 (Millipore). The value was calculated in ohms per cm^2 and the resistance of the membrane inserts only was subtracted. The unit area resistance is obtained by multiplying the electric resistance by the effective surface area of the filter.

Lentivirus. An shRNA targeting hGRHL2 (V2THS_176822) and a nonsilencing control shRNA (RHS4743) were from Thermo Scientific. To construct a Tet-on GFP-labeled dominant-negative mutant of GRHL2, DNA encoding a truncated version of mouse GRHL2 in which amino acids 1–232 were replaced with EGFP or H2B-GFP was cloned into pTRIPZ inducible lentiviral vector (Thermo Scientific) between AgeI and MluI. The vector was modified to replace RFP and insert bovine growth hormone polyA sequence after the truncated GRHL2 for its expression. Plasmids were transfected into 293T cells as described (35) using FuGENE 6 (Promega, E2691). Viral expression was confirmed by visualizing GFP after adding Dox.

Grhl3 Antibody. Rabbit polyclonal Grhl3 antibody was produced by Harlan Bioproducts for Science against amino acids 75–230 of mouse Grhl3 (83% identical to human protein). GST-Grhl3 was used for primary immunization and His-Grhl3 for boosting. The antibody was affinity-purified using His-Grhl3 and specificity was confirmed by IHC in the presence of blocking peptide.

Immunohistochemistry. Normal human lungs and ALI cultures were fixed in 4% (wt/vol) paraformaldehyde (PFA) at 4 °C for 3 h and overnight, respectively. Samples were embedded in paraffin, sectioned at 7 μm, and stained as described (36). For whole-mount staining of ALI cultures, membranes were washed with PBS and fixed with 4% PFA for 10 min at room temperature. Antibodies were rabbit GRHL1 (1:100; Sigma; HPA006420), rabbit GRHL2 (1:450; Sigma; HPA004820), rabbit Grhl3 (1:2,000), mouse monoclonal P63 (1:50; Santa Cruz; sc-8431), rabbit TJP1 (1:100; Invitrogen; 61-7300), mouse monoclonal MUC5A (1:200; Lab Vision; MS145-PO), rat CDH1 (1:500; Zymed; 13-1900), mouse acetylated tubulin (1:1,000; Sigma; T-7451), chicken GFP (1:500; Aves Labs; 1020), rabbit anti-Claudin4 (1:150; Invitrogen; 36-4800), mouse Ki67 (1:100; Vector Labs; VP-K452), and rabbit cleaved caspase 3 (1:600; Cell Signaling; 9664). Antigen retrieval on paraffin sections used 100 mM sodium citrate butter (pH 6) in a pressure cooker-like device (PickCell Laboratories; 2100 Retriever).

RNA-Seq. We performed RNA-seq on untreated, control-infected, and DN-GRHL2–infected HBE cells as described (37). For details and accession numbers, see *SI Materials and Methods*. We estimated differential expression using DESeq (38) to compare a model that included donor and condition (untreated, control-infected, or DN-infected) with a model that only accounted for donor. To be called differentially expressed, genes were required to have an FDR less than 0.05 and a more than 50% change in expression between control and DN-GRHL–infected cells. Genes were analyzed for enriched categories from Gene Ontology as described (39).

ChIP-Seq. ChIP-seq for GRHL2 was performed on HBE cells from three donors as described (40, 41) (see also *SI Materials and Methods*; Gene Expression Omnibus accession no. GSE46194). To control for sonication biases, we sequenced a matched input control library made from sonicated chromatin from each donor. We identified binding sites relative to the donor-specific input control using MACS (42). To identify reproducible GRHL2 binding sites

for our final analyses, we calculated pairwise irreproducibility discovery rates (IDRs) (43, 44) and retained binding sites with an IDR of >0.05 in all three comparisons.

Integrative ChIP-Seq and RNA-Seq Analysis. To identify genes most likely to be directly regulated by GRHL2, we identified the GRHL2 binding site nearest each RefSeq gene (42). To determine a characteristic binding distance for functional GRHL2 binding, we plotted the cumulative distribution of the distance to the nearest GRHL2 binding site for genes with increasingly significant differential expression as determined by RNA-seq. We observed a strong enrichment for GRHL2 binding within 40 kb of genes with a highly significant response to the GRHL knockdown (Fig. S2*A*). Based on this analysis, we considered differentially expressed genes within 40 kb of a GRHL2 binding site to be likely direct GRHL2 targets. To determine functional enrichment in likely direct GRHL2 target genes, we analyzed the genes for enriched categories from Gene Ontology (45) using the GOStats package (46).

Statistical Analysis of RNA-Seq and ChIP-Seq. Statistical analysis for RNA-seq and the integrative analysis with the GRHL2 ChIP-seq were performed using the R statistical package (http://www.r-project.org); a script to reproduce that analysis is available upon request. All alignment, ChIP-seq peak calling, and ChIP-seq replicate analysis were performed using publicly available software (*SI Materials and Methods*).

Microarray Analysis. RNA was extracted using an RNeasy Micro Kit (QIAGEN) and quality-checked with a 2100 Bioanalyzer (Agilent Technologies). RNA was processed using Ambion MessageAmp Premier by the Duke Microarray Facility. Standard Affymetrix protocols and human genome U133 Plus 2.0 chips were used to generate .cel files. Genomics Suite 6.5 (Partek) was used to perform data analysis. Robust multichip analysis normalization was performed on each dataset. Two-way ANOVA and fold-change analyses were performed to select target genes that were differentially expressed between control and DN-GRHL2 datasets. The top differentially expressed genes were selected with a *P*-value cutoff of <0.05 based on ANOVA test and a fold-change cutoff of >±1.5.

qRT-PCR. RNA was extracted with the RNeasy Micro Kit (QIAGEN) and cDNA was synthesized with SuperScript III (Invitrogen). PCR was performed with SYBR Green chemistry in a StepOnePlus Real-Time PCR System (Applied Biosystems). Samples were analyzed in triplicate from two or three biological replicates and data were analyzed using the ΔΔCt method (47). Primer sequences are listed in Table S1.

ACKNOWLEDGMENTS. We thank Richard Myers for support, Scott Soderling for guidance on antibody production, and Terry Lechler and Michel Bagnat for critical comments on the manuscript. This work was supported by Grant 1UO1 HL111018 (to S.H.R. and B.L.M.H.) as part of National Heart, Lung, and Blood Institute Consortium for Lung Regeneration and Repair and Core Center Grant DK06988 (to S.H.R.) for provision of primary cells.

1. Rock JR, Randell SH, Hogan BL (2010) Airway basal stem cells: A perspective on their roles in epithelial homeostasis and remodeling. *Dis Model Mech* 3(9-10):545–556.
2. Crystal RG, Randell SH, Engelhardt JF, Voynow J, Sunday ME (2008) Airway epithelial cells: Current concepts and challenges. *Proc Am Thorac Soc* 5(7):772–777.
3. Shen L, Weber CR, Raleigh DR, Yu D, Turner JR (2011) Tight junction pore and leak pathways: A dynamic duo. *Annu Rev Physiol* 73:283–309.
4. Koval M (2013) Claudin heterogeneity and control of lung tight junctions. *Annu Rev Physiol* 75:551–567.
5. Man Y, Hart VJ, Ring CJ, Sanjar S, West MR (2000) Loss of epithelial integrity resulting from E-cadherin dysfunction predisposes airway epithelial cells to adenoviral infection. *Am J Respir Cell Mol Biol* 23(5):610–617.
6. Shaykhiev R, et al. (2011) Cigarette smoking reprograms apical junctional complex molecular architecture in the human airway epithelium in vivo. *Cell Mol Life Sci* 68(5): 877–892.
7. Xiao C, et al. (2011) Defective epithelial barrier function in asthma. *J Allergy Clin Immunol* 128(3):549–556.
8. Que J, Luo X, Schwartz RJ, Hogan BL (2009) Multiple roles for Sox2 in the developing and adult mouse trachea. *Development* 136(11):1899–1907.
9. Werth M, et al. (2010) The transcription factor grainyhead-like 2 regulates the molecular composition of the epithelial apical junctional complex. *Development* 137(22): 3835–3845.
10. Hopkin AS, et al. (2012) GRHL3/GET1 and trithorax group members collaborate to activate the epidermal progenitor differentiation program. *PLoS Genet* 8(7):e1002829.
11. Wang S, Samakovlis C (2012) Grainy head and its target genes in epithelial morphogenesis and wound healing. *Curr Top Dev Biol* 98:35–63.
12. Wilanowski T, et al. (2008) Perturbed desmosomal cadherin expression in grainy head-like 1-null mice. *EMBO J* 27(6):886–897.
13. Senga K, Mostov KE, Mitaka T, Miyajima A, Tanimizu N (2012) Grainyhead-like 2 regulates epithelial morphogenesis by establishing functional tight junctions through the organization of a molecular network among claudin3, claudin4, and Rab25. *Mol Biol Cell* 23(15):2845–2855.
14. Ting SB, et al. (2005) A homolog of *Drosophila* grainy head is essential for epidermal integrity in mice. *Science* 308(5720):411–413.
15. Auden A, et al. (2006) Spatial and temporal expression of the Grainyhead-like transcription factor family during murine development. *Gene Expr Patterns* 6(8):964–970.
16. Varma S, et al. (2012) The transcription factors Grainyhead-like 2 and NK2-homeobox 1 form a regulatory loop that coordinates lung epithelial cell morphogenesis and differentiation. *J Biol Chem* 287(44):37282–37295.
17. Pyrgaki C, Liu A, Niswander L (2011) Grainyhead-like 2 regulates neural tube closure and adhesion molecule expression during neural fold fusion. *Dev Biol* 353(1):38–49.
18. Pezzulo AA, et al. (2011) The air-liquid interface and use of primary cell cultures are important to recapitulate the transcriptional profile of in vivo airway epithelia. *Am J Physiol Lung Cell Mol Physiol* 300(1):L25–L31.
19. Bhandari A, et al. (2013) The Grainyhead transcription factor Grhl3/Get1 suppresses miR-21 expression and tumorigenesis in skin: Modulation of the miR-21 target MSH2 by RNA-binding protein DND1. *Oncogene* 32(12):1497–1507.
20. McLean CY, et al. (2010) GREAT improves functional interpretation of *cis*-regulatory regions. *Nat Biotechnol* 28(5):495–501.
21. Bauer H, Zweimueller-Mayer J, Steinbacher P, Lametschwandtner A, Bauer HC (2010) The dual role of zonula occludens (ZO) proteins. *J Biomed Biotechnol* 2010:402593.
22. Cheng TL, et al. (2011) Functions of rhomboid family protease RHBDL2 and thrombomodulin in wound healing. *J Invest Dermatol* 131(12):2486–2494.
23. Tarbé NG, Rio MC, Weidle UH (2004) SMAGP, a new small trans-membrane glycoprotein altered in cancer. *Oncogene* 23(19):3395–3403.
24. Ding X, Jiang QB, Li R, Chen S, Zhang S (2012) NOK/STYK1 has a strong tendency towards forming aggregates and colocalises with epidermal growth factor receptor in endosomes. *Biochem Biophys Res Commun* 421(3):468–473.
25. Caddy J, et al. (2010) Epidermal wound repair is regulated by the planar cell polarity signaling pathway. *Dev Cell* 19(1):138–147.
26. Liu JY, et al. (2009) Vav proteins are necessary for correct differentiation of mouse cecal and colonic enterocytes. *J Cell Sci* 122(Pt 3):324–334.
27. Willems A, et al. (2010) Selective ablation of the androgen receptor in mouse Sertoli cells affects Sertoli cell maturation, barrier formation and cytoskeletal development. *PLoS One* 5(11):e14168.
28. Brancati F, et al. (2010) Mutations in PVRL4, encoding cell adhesion molecule nectin-4, cause ectodermal dysplasia-syndactyly syndrome. *Am J Hum Genet* 87(2):265–273.
29. Shapiro IM, et al. (2011) An EMT-driven alternative splicing program occurs in human breast cancer and modulates cellular phenotype. *PLoS Genet* 7(8):e1002218.
30. Faucheux C, et al. (2010) Vestigial like gene family expression in *Xenopus*: Common and divergent features with other vertebrates. *Int J Dev Biol* 54(8-9):1375–1382.
31. Cohen I, et al. (2012) ZNF750 is expressed in differentiated keratinocytes and regulates epidermal late differentiation genes. *PLoS One* 7(8):e42628.
32. Francis SM, et al. (2009) Expression profiling identifies genes involved in emphysema severity. *Respir Res* 10:81.
33. Singer S, et al. (2009) Coordinated expression of stathmin family members by far upstream sequence element-binding protein-1 increases motility in non-small cell lung cancer. *Cancer Res* 69(6):2234–2243.
34. Fulcher ML, Gabriel S, Burns KA, Yankaskas JR, Randell SH (2005) Well-differentiated human airway epithelial cell cultures. *Methods Mol Med* 107:183–206.
35. Dull T, et al. (1998) A third-generation lentivirus vector with a conditional packaging system. *J Virol* 72:8463–8471.
36. Rock JR, et al. (2011) Notch-dependent differentiation of adult airway basal stem cells. *Cell Stem Cell* 8(6):639–648.
37. Gertz J, et al. (2012) Transposase mediated construction of RNA-seq libraries. *Genome Res* 22(1):134–141.
38. Anders S, Huber W (2010) Differential expression analysis for sequence count data. *Genome Biol* 11(10):R106.
39. Beissbarth T, Speed TP (2004) GOstat: Find statistically overrepresented Gene Ontologies within a group of genes. *Bioinformatics* 20(9):1464–1465.
40. Johnson DS, Mortazavi A, Myers RM, Wold B (2007) Genome-wide mapping of in vivo protein-DNA interactions. *Science* 316(5830):1497–1502.
41. Reddy TE, et al. (2012) Effects of sequence variation on differential allelic transcription factor occupancy and gene expression. *Genome Res* 22(5):860–869.
42. Zhang Y, et al. (2008) Model-based analysis of ChIP-Seq (MACS). *Genome Biol* 9(9): R137.
43. Li Q, Brown JB, Huang HH, Bickel PJ (2011) Measuring reproducibility of high-throughput experiments. *Ann Appl Stat* 5(3):1752–1779.
44. Landt SG, et al. (2012) ChIP-seq guidelines and practices of the ENCODE and modENCODE consortia. *Genome Res* 22(9):1813–1831.
45. Ashburner M, et al.; The Gene Ontology Consortium (2000) Gene Ontology: Tool for the unification of biology. *Nat Genet* 25(1):25–29.
46. Falcon S, Gentleman R (2007) Using GOstats to test gene lists for GO term association. *Bioinformatics* 23(2):257–258.
47. Livak KJ, Schmittgen TD (2001) Analysis of relative gene expression data using real-time quantitative PCR and the 2(-Delta Delta c(T)) Method. *Methods* 25(4):402–408.